

## The young surface of (50000) Quaoar

M. A. Barucci (1), C. M. Dalle Ore (2), D. Perna (1), D. P. Cruikshank (2), A. Doressoundiram (1), A. Alvarez-Candal (3), E. Dotto (4), and C. Nitschelm (5)

(1) LESIA – Observatoire de Paris, CNRS, UPMC Univ. Paris 06, Univ. Paris-Diderot, 5 place J. Janssen, 92195, Meudon, France (antonella.barucci@obspm.fr / Fax : +33 145077144), (2) NASA Ames Research Center, Mail Stop 245-6, Moffett Field, CA 94035, USA, (3) Observatorio Nacional, Rio de Janeiro, Brazil, (4) INAF-Osservatorio di Monteporzio, Roma, Italy, (5) Unidad de Astronomía, Facultad de Ciencias Básicas, Universidad de Antofagasta, Antofagasta, Chile

### Abstract

We present new continuous spectra from visible to near-infrared (0.3-2.3  $\mu\text{m}$ ) obtained with the X-Shooter instrument at the VLT-ESO at four different epochs on the surface of Quaoar. The data are complemented by previously published photometric observations obtained in the near-infrared (3.6, 4.5  $\mu\text{m}$ ) with the Spitzer Space Telescope. Spectral modeling was performed for the entire wavelength range by means of a code based on the Shkuratov radiative transfer formulation and using an updated value of albedo obtained from Herschel observations.

### 1. Introduction

(50000) Quaoar is one of the largest classical transneptunian objects in a binary system, with a recent diameter determination of  $1036 \pm 31$  km and an albedo of 12.7% [1] obtained with Herschel observations together with revised Spitzer data. Quaoar is also a very red object, classified as RR type [2] for its red spectral slope. It also appears to be rich in more complex irradiation products.

New observations were performed in August 2013 at the ESO-VLT using a new generation spectrograph X-Shooter recording simultaneously from ultraviolet to near-infrared (0.3-2.3  $\mu\text{m}$ ) wavelengths. The data obtained at different rotational phases are complemented by previously published photometric data [3] in the near-infrared (at 3.6, 4.5  $\mu\text{m}$ ) obtained with the Spitzer Space Telescope. Along with the updated visible albedo [1] the Spitzer data provide an

extra set of constraints in the model calculation process. For the new four spectra we perform spectral modeling first of the wavelength range from 0.3 to 2.3  $\mu\text{m}$  and then adding the Spitzer data for extra constraints. We make use of a code based on the Shkuratov et al. [4] radiative transfer formulation of the slab model.

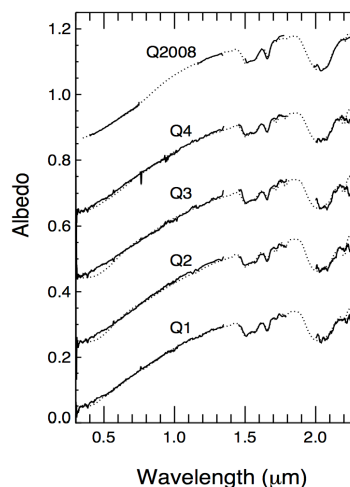


Figure 1: Five spectra of (50000) Quaoar (solid lines) are shown with their corresponding spectral models (dotted lines). Spectra labeled Q1 through Q4 are newly obtained, while Q2008 is from previous observations [3]. The top four spectra have been shifted by +0.2, +0.4, +0.6 and +0.8 units for clarity.

## 2. Observations and analysis

We present new visible to near-infrared (0.3-2.3  $\mu\text{m}$ ) spectral data obtained with the X-Shooter at the VLT-ESO at four different epochs on the surface of Quaoar. The newly obtained data cover about 40% of the object's rotation, with the assumption that the rotational period is 8.84 hrs [5]. The observations show a strong similarity as reported in Fig. 1 (Q1-Q4 spectra) which implies homogeneity of the surface composition on one hemisphere of Quaoar. This is also confirmed by the best fitting models calculated with a radiative transfer code [4]. Spitzer IRAC data [3] were also included with the new spectral data to better constrain the composition of the surface (Fig. 2). The best fitting model is reported in Table 1.

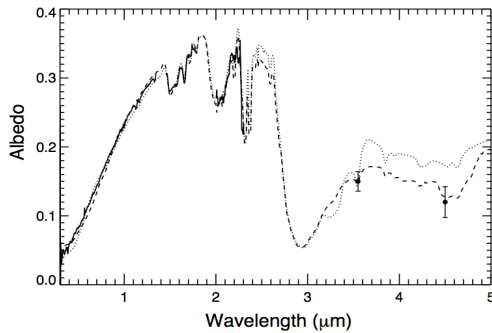


Figure 2: Spectrum of Quaoar (Q2, solid line) with Spitzer photometry (black dots) and corresponding best fitting spectral model (dashed line, parameters are listed in Table 1) that includes CO diluted in N<sub>2</sub> and CO<sub>2</sub>. The best fitting model for the spectral dataset, without CO and CO<sub>2</sub>, is also shown for comparison (dotted line).

## 6. Conclusions

Quaoar's visible spectral red slope is best matched by the inclusion of Triton and Titan tholin. H<sub>2</sub>O ice in its crystalline phase is also clearly present. Quaoar's surface composition is partly inferred from the shifts of the CH<sub>4</sub> bands, as expected when this material is embedded in a N<sub>2</sub> matrix. Like CO in N<sub>2</sub>, CO<sub>2</sub> is also included in the model only as an upper limit necessary to match the data at the two Spitzer bands. The comparison between the old Q2008 model and the new ones offers further evidence in favor of the presence of diluted CO and CO<sub>2</sub> on Quaoar. In the old model very small H<sub>2</sub>O ice grains had to be

adopted to fit the Spitzer data. With the inclusion of CO in N<sub>2</sub> and CO<sub>2</sub> this is no longer necessary.

The presence of crystalline H<sub>2</sub>O ice and NH<sub>4</sub>OH on the surface of Quaoar, may indicate an efficient renewal mechanism in favor of the hypothesis of a young surface. Numerical simulations [6] describing the thermal evolution of TNOs as function of the intensity of radiogenic heat, predicts the possible presence of cryovolcanism on Quaoar. Alternatively, crystalline H<sub>2</sub>O ice could be the product of impact gardening and NH<sub>4</sub>OH could be seeping up to the surface of Quaoar by a diffusive mechanism.

The spectrum of Quaoar is consistent with that of a cold object slowly losing the last of its volatile ices by escape to a tenuous atmosphere.

Table 1: Best fit of the Quaoar spectrum and the Spitzer data

Components	Q2+Spitzer
Titan tholin in CH <sub>4</sub>	0.13
Triton tholin in CH <sub>4</sub>	0.09
Triton tholin in H <sub>2</sub> O	0.08
H <sub>2</sub> O cryst (40K)	0.07(18)
C <sub>2</sub> H <sub>6</sub> in N <sub>2</sub>	0.02(31)
Triton tholin	0.36(7)
N <sub>2</sub> (36-60K)	0.03(1610)
CH <sub>4</sub> in N <sub>2</sub>	0.21(80)
CO in N <sub>2</sub>	0.05(150)
AC	0.11(20)
CO <sub>2</sub>	0.04(100)
NH <sub>4</sub> OH	0.12(65)

## References

- [1] Fornasier, S., Lellouch, E., Muller, T. et al. 2013, A&A 555, A15
- [2] Barucci, M. A., Belskaya, I. Fulchignoni, M. et al. 2005, AJ, 130, 1291
- [3] Dalle Ore C.M., Barucci, M. A., Emery, J.P. et al. 2009, A&A, 501, 349
- [4] Shkuratov, Y., Starukhina, L., Hoffmann, H., & Arnold, G. 1999, Icarus, 137, 235
- [5] Thirouin A., Ortiz J., Dufard R. et al. 2010, A&A, 522, A93
- [6] Shchuko O.B., Shchuko S.D., Kartashov D.V., and Orosei R. 2014, PSS, 104,147